Situation Awareness and Sensitivity Analysis for Absorption of Grid-connected Renewable Energy Power Generation Integrating Robust Optimization and Radial Basis Function Neural Network

Ziqi Zhang, Zhong Chen, Qi Zhao, Yi Wang, and Jiang Tian

***Abstract*—The significance of situation awareness (SA) in power systems has increased to enhance the utilization of grid-connected renewable energy power generation (REPG). This paper proposes a real-time calculation architecture based on the integration of robust optimization (RO) and artificial intelligence. First, the time-series simulation of the REPG consumption capacity is carried out under the current grid operating conditions. RO is employed in this simulation, given the randomness of the REPG output and the grid load. Then, the radial basis function neural network (RBFNN) is trained with the results under different parameters using the artificial fish swarm algorithm (AFSA), enabling the neural network (NN) to be the replacement for the time-series simulation model. The trained NN can quickly perceive the REPG absorption situation within the predefined grid structure and period. Moreover, the Sobol' method is adopted to conduct the global sensitivity analysis for different parameters based on the input-output samples obtained by the trained NN. Finally, the simulation experiments based on the modified IEEE 14-bus system prove the real-time performance and accuracy of the proposed SA architecture.**

***Index Terms*—Renewable energy, radial basis function neural network, robust optimization, sensitivity analysis, situation awareness.**

I. Introduction

THE injection of renewable energy power generation (REPG) into the power grid is crucial for improving energy security and achieving carbon neutrality [1], [2]. However, the volatility and randomness of wind power (WP) and photovoltaic (PV) present a significant challenge for system operators who must ensure the efficient and safe absorption of the grid-connected REPG while maintaining the economic and operational stability of the power grid [3]-[5].

The direct consequence of insufficient consumption of the REPG is electricity curtailment. In 2019, the curtailment in China and Germany reached 16869 GWh and 6273 GWh [6], respectively, resulting in more than 1 billion euros in economic losses. Quantitative evaluation of the REPG consumption capacity based on the parameters of the current power grid can provide the maximum limit for the REPG of a specific power system and guide the construction of renewable energy sources [7], [8]. Moreover, identifying the key parameters that affect the REPG absorption can help guide the grid operation and the electricity market [9] to improve the consumption rate (CR) on various time scales. Thus, numerous research works have been conducted on the evaluation means including multi-scenario, probabilistic, and time-series simulations.

An absorption analysis based on stochastic scenarios for WP is proposed in [10], which considers the correlation between WP and grid load. Reference [11] develops the correlation between WP and PV and employs the Copula model to analyze various scenarios. In [12], the frequency stability is taken as a constraint to calculate the absorption capacity for the typical days. The probabilistic power flow inspires and provides the theoretical basis for the probabilistic method [13]-[16]. The absorption results can be calculated directly according to the probability distribution of the load and REPG output. The time-series simulation has been the most widely used method in analyzing REPG absorption for accuracy [17]-[22]. Reference [17] combines the day-ahead unit commitment, which employs WP's quadratic optimization (considering the costs of conventional units), with the absorption capacity assessment for a long period. A Nordic power system model is constructed in [18] to study the curtailment of the WP in 2025 based on historical data, and the influencing factors such as the transmission line capacity (TLC) are analyzed. The concept of the contribution degree for REPG accommodation factors is constructed in [20] to discover the interaction between various parameters. Then, the amount of REPG curtailment is calculated under differ-

Manuscript received: October 9, 2022; revised: February 12, 2023; accepted: March 31, 2023. Date of CrossCheck: March 31, 2023. Date of online publication: May 4, 2023.

This work was supported in part by the National Natural Science Foundation of China (No. 52077035).

Z. Zhang and Z. Chen (corresponding author) are with the School of Electrical Engineering, Southeast University, Nanjing, China (e-mail: zqzhang_ee@seu.edu.cn; chenzhong_seu@163.com).

Q. Zhao and J. Tian are with the Suzhou Power Supply Branch of the State Grid Jiangsu Electric Power Company, Suzhou, China (e-mail: zqsz2021@163.com; 18829886111@139.com).

Y. Wang is with NARI Group Corporation Ltd., (State Grid Electric Power Research Institute Ltd.,), Nanjing, China (e-mail: wang-yi2@sgepri.sgcc.com.cn).

DOI: 10.35833/MPCE.2022.000683

ent conditions.

The above methods all have shortcomings. The calculation results of the multi-scenario method do not consider the timing characteristics of the power system, and the probabilistic method cannot incorporate some essential constraints such as the ramping rate of the conventional units. In addition, since the span of the time-series simulation is usually more than one year and some iterations may be required, the calculation time can be pretty long. Although the time-series simulation results can guide offline planning, this method cannot be applied to online situation awareness (SA), which supports the scheduling decision [23]. Moreover, sensitivity analysis to identify critical factors affecting the REPG absorption requires massive sample data, which are difficult to obtain through time-series simulation because of its long calculation time.

The probabilistic method has revealed the existence of an analytical relationship between the absorption results and the parameters that influence the REPG absorption in a specified power grid and during a specified period [13], [16]. This high-dimensional and nonlinear mathematical relationship can be effectively fitted by the neural network (NN) [24], presenting a novel method for rapidly calculating absorption results. Therefore, this paper proposes an architecture that combines the NN and time-series simulation for online SA and sensitivity analysis of REPG absorption. The utilization of machine learning provides two advantages. Firstly, the NN can calculate the absorption of the next time window and perceive the trend over an extended period, enabling it to provide useful guidance for the system operator. Additionally, the NN can perform sample expansion based on the time-series simulation results, providing sufficient samples for global sensitivity analysis. Figure 1 shows the main contributions of this paper.

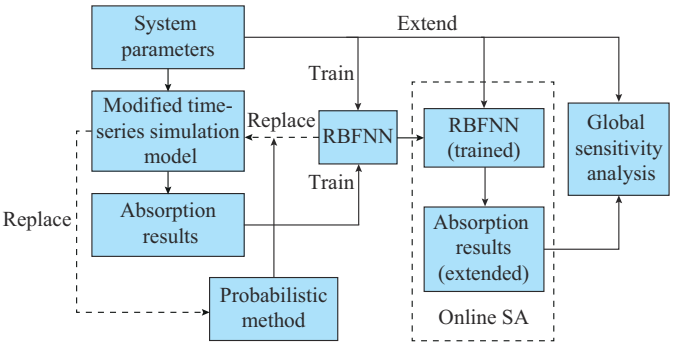

Fig. 1. Main contributions of this paper.

1) We address the volatility and randomness of the REPG and load by developing a time-series simulation model based on robust optimization (RO). We change input parameters to obtain simulation results under various conditions. These samples are then used to train a radial basis function neural network (RBFNN) employing the artificial fish swarm algorithm (AFSA). The trained NN can accurately predict real-time absorption results within the set grid.

2) We carry out the global sensitivity analysis using Sobol' method to investigate the impact of different parameters on the absorption results. This method considers the interaction between various parameters based on variance [25], unlike the the local sensitivity analysis which only utilizes the first-order partial differential of the output to the input. To ensure the convergence of sensitivity analysis, we adopt the trained RBFNN to expand the results of the time-series simulation so that enough samples can be available.

The rest of this paper is organized as follows. Section II develops the time-series simulation based on RO. Section III proposes the online SA based on AFSA-RBFNN. Section IV introduces the global sensitivity analysis of REPG absorption by Sobol' method. Section V conducts the simulation experiments, and Section VI summarizes the paper.

II. Time-series Simulation Based on RO

While the current work based on the time-series simulation has considered the volatility of the REPG, the randomness is often neglected. It is imperative to note that the REPG output cannot be regarded as a definitive curve in the day-ahead unit commitment since it is not entirely predictable. Although the reserve capacity of conventional power generation can cover some prediction errors, the optimized results could not meet the up/down ramping constraint, resulting in the curtailment of the REPG and the loss of load [26]. This may, in turn, lead to imprecise assessment results. This section proposes an time-series simulation based on RO that considers the worst-case condition to achieve optimal results while including the influence of the volatility and randomness of the REPG on the absorption. Although this method requires a longer calculation time, it can provide better samples for NN training. To the best of our knowledge, there are few reports on the application of RO in the time-series simulation for REPG absorption.

A. Process and Objective Function of Simulation

Figure 2 demonstrates the process of the time-series simulation based on RO. After setting the grid topology and other initial parameters, the RO will be carried out consecutively in each time window (one day in this paper). Then, we record the optimization results and the boundary conditions such as the output and state of conventional generation that will be transferred to the next time window.

The objective function is given as:

$$\min_{P_t^{\mathrm{PV}} \in \mathcal{P}_t^{\mathrm{PV}}, P_t^{\mathrm{WT}} \in \mathcal{P}_t^{\mathrm{WT}}, P_t^{\mathrm{L}} \in \mathcal{P}_t^{\mathrm{L}}} \sum_{t=1}^{NT} \sum_{i=1}^{NG} P_{i,t}^{\mathrm{G}} \tag{1}$$

where $P_{i,t}^{\mathrm{G}}$ is the output of conventional generation i in time interval t; NG is the number of conventional units; NT is the value of time intervals in each time window; P_t^{PV} and P_t^{WT} are the maximum outputs of PV and WP in time interval t, respectively, which have uncertainties; $\mathcal{P}_t^{\mathrm{PV}}$ and $\mathcal{P}_t^{\mathrm{WT}}$ are the sets of their possible values, respectively; and P_t^{L} is the random value of grid load in time interval t, while $\mathcal{P}_t^{\mathrm{L}}$ is the set of its values. Reducing the power of conventional generations can promote the REPG utilization, so the curtailment of WP and PV can be lower.

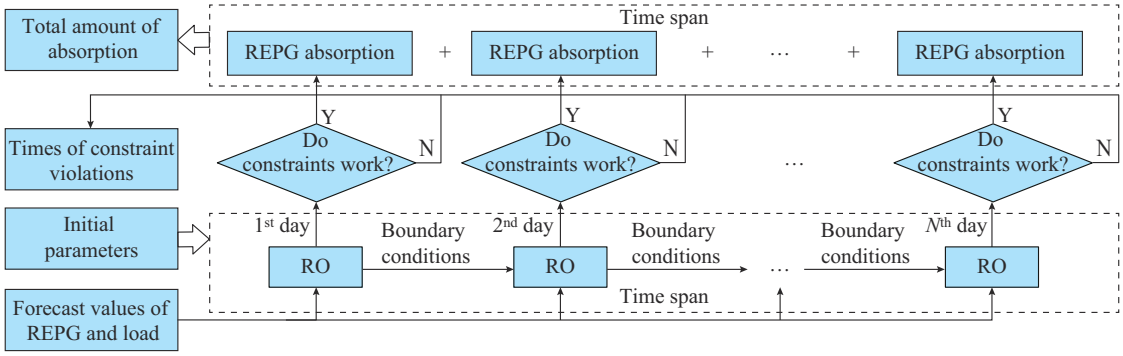

Fig. 2. Process of time-series simulation based on RO.

B. Constraints

1) Conventional Generation

Constraints of the conventional generations include the max-min output, ramping capacity, and on-off time:

$$P^{\mathrm{G}}_{i,\min} s^{\mathrm{G}}_{i,t} \le P^{\mathrm{G}}_{i,t} \le P^{\mathrm{G}}_{i,\max} s^{\mathrm{G}}_{i,t} \tag{2}$$

$$\begin{cases} P^{\mathrm{G}}_{i,t+1} - P^{\mathrm{G}}_{i,t} \le P^{\mathrm{G,up}}_{i} \\ P^{\mathrm{G}}_{i,t} - P^{\mathrm{G}}_{i,t+1} \le P^{\mathrm{G,down}}_{i} \end{cases} \tag{3}$$

$$\begin{cases} X^{\mathrm{G}}_{i,t} + \sum_{j=1}^{T_{\mathrm{on}}} Y^{\mathrm{G}}_{i,t+j} \le 1 \\ Y^{\mathrm{G}}_{i,t} + \sum_{j=1}^{T_{\mathrm{off}}} X^{\mathrm{G}}_{i,t+j} \le 1 \end{cases} \tag{4}$$

$$\begin{cases} s^{\mathrm{G}}_{i,t} - s^{\mathrm{G}}_{i,t-1} - X^{\mathrm{G}}_{i,t} + Y^{\mathrm{G}}_{i,t} = 0 \\ -s^{\mathrm{G}}_{i,t} - s^{\mathrm{G}}_{i,t-1} + X^{\mathrm{G}}_{i,t} \le 0 \\ s^{\mathrm{G}}_{i,t} + s^{\mathrm{G}}_{i,t-1} + X^{\mathrm{G}}_{i,t} \le 2 \\ -s^{\mathrm{G}}_{i,t} - s^{\mathrm{G}}_{i,t-1} + Y^{\mathrm{G}}_{i,t} \le 0 \\ s^{\mathrm{G}}_{i,t} + s^{\mathrm{G}}_{i,t-1} + Y^{\mathrm{G}}_{i,t} \le 2 \end{cases} \tag{5}$$

where $P^{\mathrm{G}}_{i,\max}$ and $P^{\mathrm{G}}_{i,\min}$ are the maximum and minimum outputs of generation i, respectively; $s^{\mathrm{G}}_{i,t}$ is a binary variable representing the on-off states of generation i in time interval t as 1-0; $P^{\mathrm{G,up}}_{i}$ and $P^{\mathrm{G,down}}_{i}$ are the maximum ramping up and ramping down capacities, respectively; $X^{\mathrm{G}}_{i,t}$ and $Y^{\mathrm{G}}_{i,t}$ are the binary variables, and generation i will start or halt in time interval t if $X^{\mathrm{G}}_{i,t}$ or $Y^{\mathrm{G}}_{i,t}$ equals 1; and T_{on} and T_{off} are the shortest durations of consecutive on and off states, respectively. Formula (5) constrains the logical relationships between start-up, shutdown, and on-off states.

2) REPG Output

In (6), P^{PV}_{t} and P^{WT}_{t} are supposed to be no more than the maximum prediction values.

$$\begin{cases} 0 \le P^{\mathrm{PV}}_{t} \le \mathcal{P}^{\mathrm{PV}}_{t} \\ 0 \le P^{\mathrm{WT}}_{t} \le \mathcal{P}^{\mathrm{WT}}_{t} \end{cases} \tag{6}$$

3) Power Balance and Spinning Reserve

Formula (7) ensures that the total output of the REPG and conventional units is greater than the grid load, even in the worst scenario. Formula (8) is the spinning reserve constraint in which P_{re} is the reserved capacity.

$$\sum_{i=1}^{NT} P^{\mathrm{G}}_{i,t} + P^{\mathrm{PV}}_{t} + P^{\mathrm{WT}}_{t} \ge P^{\mathrm{L}}_{t} \tag{7}$$

$$\sum_{i=1}^{NT} P^{\mathrm{G}}_{i,\max} s^{\mathrm{G}}_{i,t} + P^{\mathrm{PV}}_{t} + P^{\mathrm{WT}}_{t} - P^{\mathrm{L}}_{t} \ge P_{\mathrm{re}} \tag{8}$$

4) TLC

The power flow transfer factor γ_{l-b} is adopted to depict the influence of node b on the power flow of line l.

$$-T_{l,\max} \le \sum_{b=1}^{N_b} \gamma_{l-b} P_{b,t} \le T_{l,\max} \tag{9}$$

where N_b is the number of grid nodes; and $T_{l,\max}$ is the maximum TLC of line l.

We regard the parameters related to the REPG and load as random variables in RO. When these parameters change within a specific range, all the constraints should still be satisfied. RO is an NP-hard problem but can be calculated using the algorithms such as column and constraint generation (C&CG) [27]. However, to evaluate the future trend of REPG absorption, the time-series simulation based on RO is not only carried out for the next single time window but repeated in numerous time windows. Hence, although C&CG can complete RO within a second, the total simulation time may be unacceptable for online applications.

III. Online SA Based on AFSA-RBFNN

A. Framework of Integration of RO and NN

The limitation of the time-series simulation is its extended computational time for online scheduling decision support and generation of a significant number of samples, which are essential for global sensitivity analysis. Hence, based on the time-series simulation, this subsection develops a method for online SA toward the REPG absorption employing NN. The framework of the NN-based online SA is illustrated in Fig. 3.

First, the parameters that may influence REPG absorption will be input into the time-series simulation based on RO. We select ten parameters in this paper: prediction error of load (PEL), peak load (PL), peak-valley difference of load (PVDL), amount of flexible load (AFL), TLC, REPG capacity (REC), prediction error of REPG (PERE), capacity of conventional generation (CCG), minimum output of conventional generation (MICG), and ramping rate of conventional generation (RRCG). Then, the absorption results will be calculated for the specified grid and period. We can obtain multiple input-output data sets as training samples by adjusting the parameters.

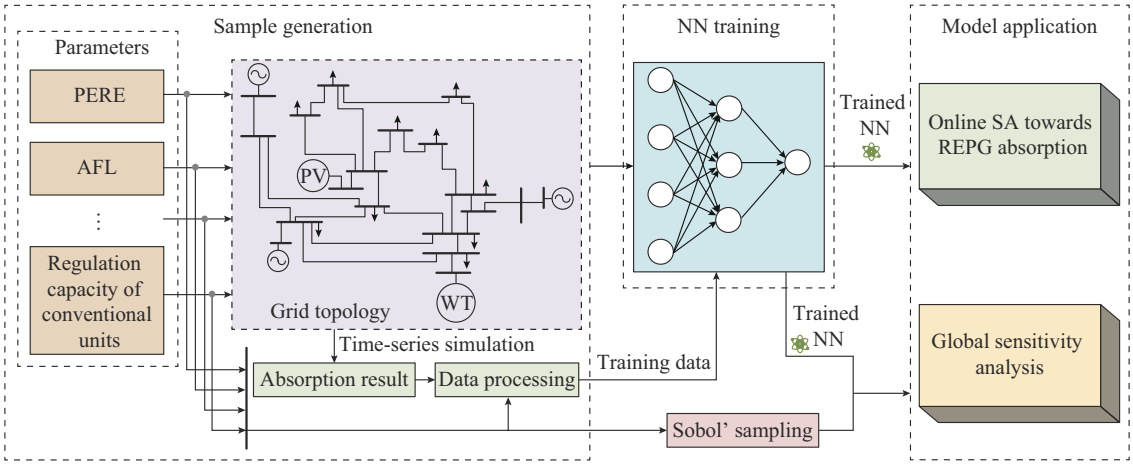

Fig. 3. Framework of NN-based online SA.

Second, the RBFNN will be trained based on the samples acquired from the time-series simulation. Thus, the trained RBFNN can perceive the REPG absorption results of the prescribed power grid during the specified period according to the characteristic parameters.

Finally, we generate a large number of parameter sets through Sobol' sampling. The corresponding absorption results can be achieved based on the trained RBFNN, which provides numerous samples for global sensitivity analysis. Therefore, we can quantitatively reveal the comprehensive influence of various characteristic parameters on REPG absorption.

B. AFSA-RBFNN Training Method

Artificial NNs have emerged as a powerful tool in the research and practice of power systems. The specific tasks determine the form of NN utilized. For example, long short-term memory (LSTM) NN, which can effectively process time series, is good at forecasting load and REPG output [28]. Networks such as stacked autoencoder (SAE) and self-organizing map (SOM) can solve classification problems such as the transient stability assessment for their ability of feature extraction [29]. In this paper, we want to fit the high-dimensional, continuous, and nonlinear relationships of the input parameters and output results of the time-series simulation based on RO. Therefore, RBFNN is adopted. RBFNN employs the radial basis function in the hidden layer and projects the low-dimensional input vector to the high-dimensional space so that the original linear indivisible problems can become linearly separable. Because of its strong generalization ability, fast convergence speed, and good local approximation performance [30], [31], RBFNN has been widely used in time-series forecasting [32], nonlinear optimization [33], and pattern recognition [34]. Moreover, to improve the fitting accuracy, AFSA [35], [36] is employed to optimize the initial NN parameters.

We utilize the Gaussian kernel function as the activation function:

$$\phi_k(\mu)=\exp\left(-\frac{\left\|\boldsymbol{\mu}_k-\boldsymbol{c}_k\right\|^2}{2\boldsymbol{d}_k^2}\right) \tag{10}$$

where $\boldsymbol{\mu}_k$ is the input sample; and $\boldsymbol{c}_k$ and $\boldsymbol{d}_k$ are the center vector and the neuron width of the hidden layer, respectively. The output result v is the sum of the products of the weight vectors $\boldsymbol{\omega}_m$ and the corresponding $\phi_k(\mu)$.

$\boldsymbol{c}_k$, $\boldsymbol{d}_k$, and $\boldsymbol{\omega}_m$ are the crucial parameters of RBFNN, of which the general training method can be found in [30]. To further reduce the error of training results, we will search for the optimal initial values of parameters based on AFSA. Figure 4 presents the AFSA-RBFNN training method.

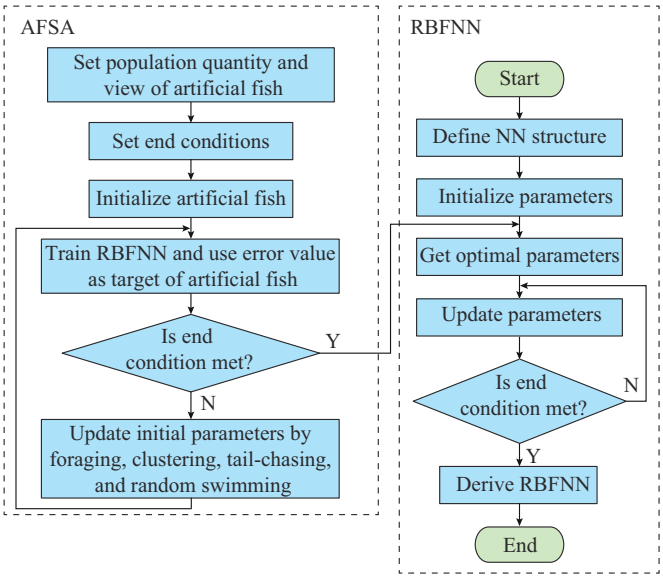

Fig. 4. AFSA-RBFNN training method.

IV. Global Sensitivity Analysis of REPG Absorption by Sobol' Method

Sobol' method finds wide application in the fields such as economy, environment, and society [37]. Moreover, it has been applied in voltage stabilization [38], minor disturbance stabilization [39], and distributed energy system design [40]. However, there have been no related reports about its application in REPG absorption.

The global sensitivity analysis can obtain the independent influence of different parameters on the absorption results

and consider each parameter's effect when coupled with the others. The Sobol' method conducts the global sensitivity analysis based on variance, calculated by decomposing the input-output function $f(\boldsymbol{\mu})$ as:

$$f(\mu_1,\mu_2,\ldots,\mu_K)=f_0+\sum_{k=1}^{K}f_k(\mu_k)+\sum_{1\le k_1<k_2\le K}f_{k_1k_2}(\mu_{k_1},\mu_{k_2})+\ldots+f_{1,2,\ldots,K}(\mu_1,\mu_2,\ldots,\mu_K) \tag{11}$$

The sensitivity coefficient can be expressed as:

$$S_{k_1,k_2,\ldots,k_s}=\frac{D_{k_1,k_2,\ldots,k_s}}{D} \tag{12}$$

where D is the total variance; and $D_{k_1,k_2,\ldots,k_s}$ is the partial variance caused by various parameters $(1\le k_1<\ldots<k_s\le K)$; S_k is the first-order sensitivity coefficient of parameter k; and S_{k_1,k_2} is the second-order sensitivity coefficient which represents the cross-influence of k_1 and k_2. The total sensitivity coefficient of k equals the sum of its various orders.

Based on (11) and (12), to calculate the first-order and total sensitivity coefficients of each parameter, the variance is then estimated by Monte Carlo simulation according to (13):

$$\begin{cases}\hat{f}_0=\dfrac{1}{N}\displaystyle\sum_{m=1}^{N}f(\boldsymbol{\mu}_m)\\ \hat{D}=\dfrac{1}{N}\displaystyle\sum_{m=1}^{N}f^2(\boldsymbol{\mu}_m)-\hat{f}_0^2\\ \hat{D}_k=\dfrac{1}{N}\displaystyle\sum_{m=1}^{N}f(\boldsymbol{\mu}^{(1)}_{m(\sim k)},\boldsymbol{\mu}^{(1)}_{mk})f(\boldsymbol{\mu}^{(2)}_{m(\sim k)},\boldsymbol{\mu}^{(1)}_{mk})-\hat{f}_0^2\\ \hat{D}_{\sim k}=\dfrac{1}{N}\displaystyle\sum_{m=1}^{N}f(\boldsymbol{\mu}^{(1)}_{m(\sim k)},\boldsymbol{\mu}^{(1)}_{mk})f(\boldsymbol{\mu}^{(1)}_{m(\sim k)},\boldsymbol{\mu}^{(2)}_{mk})-\hat{f}_0^2\end{cases} \tag{13}$$

where N is the number of samples; the superscripts (1) and (2) represent two $N\times K$ dimensional sampling matrices; $\boldsymbol{\mu}_{m(\sim k)}$ represents all columns of matrix $\boldsymbol{\mu}_m$ without the sampled values of parameter k; $\hat{D}_{\sim k}$ is the estimated value of variance caused by changes of parameters except k; and $\hat{}$ represents the estimated value. Therefore, the total sensitivity coefficient of k is given as:

$$TS_k=1-\frac{\hat{D}_{\sim k}}{\hat{D}} \tag{14}$$

Figure 5 shows the Sobol' sampling based global sensitivity analysis.

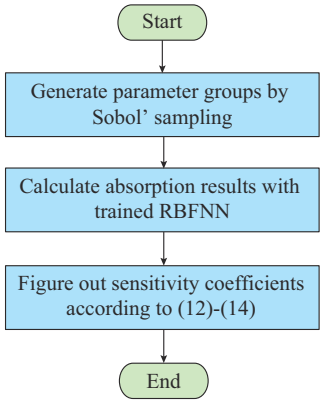

Fig. 5. Sobol' sampling based global sensitivity analysis.

V. Case Study

A. Comparison Between Results of Time-series Simulation Based on Robust and Deterministic Optimization

The time-series simulations are based on a modified IEEE 14-bus system presented in Fig. 6. We list the parameters in the Supplementary Material, including the admittance matrix and the power flow transfer factors, as shown in Tables SAI and SAII. We set the simulation period as one year, and the time window is one day with 1-hour interval, so 365 time windows are considered during RO. The curves of the REPG output and the grid load are the actual data on the southeast coast of China in 2020, as shown in Figs. SA1-SA3 in the Supplementary Material. The maximum load is supposed to be 220 MW, and the maximum outputs of WP and PV are 77 MW and 33 MW, respectively. We set the total maximum output of conventional generations to be 240 MW, and the other parameters of these generations are in Table SAIII.

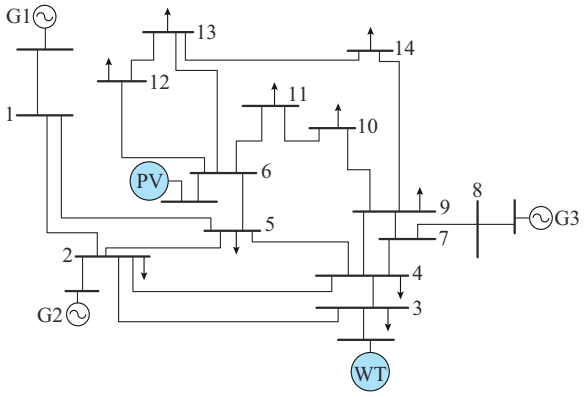

Fig. 6. Modified IEEE 14-bus system.

In the time-series simulation based on RO, the uncertainties of the PV output, the WP output, and the grid load are considered, unlike in the time-series simulation based on deterministic optimization, where the predicted value is directly used as input parameters for each optimization. Figure 7 illustrates the curves and uncertain ranges of REPG output and grid load. The possible range of uncertain parameters is taken as ±5% of the prediction values.

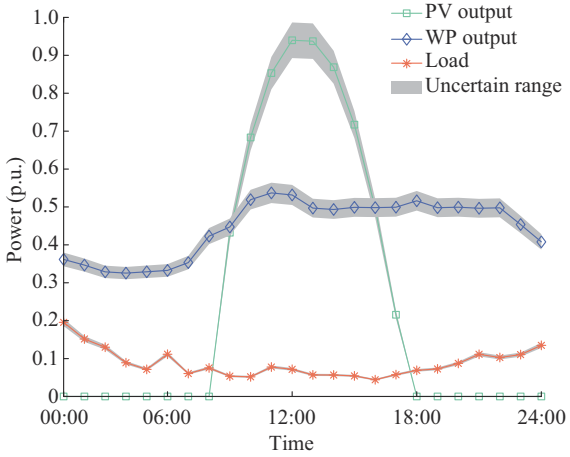

Fig. 7. Curves and uncertain ranges of REPG output and grid load.

Constraint violations must occur during this time window if the RO model cannot be solved successfully. In such cases, the REPG CR of this time window is regarded as zero, and the number of times this situation occurs is conunted during the whole simulation span.

We conducted all experiments on a personal computer with an Intel Core i7-9700 CPU and 32 GB of RAM using MATLAB 2019a with MOSEK. The time-series simulation based on RO took 192.62 s, while the deterministic algorithm only took 52.12 s. The simulation considering randomness needs more calculation time for its complexity.

The REPG CR derived by the RO algorithm is 71.41%, and the constraints are violated 23 times. However, the CR is 94.46% with the deterministic optimization-based simulation, where the constraint violations occur only ten times. Figure 8 presents histograms of the CRs in various time windows. The deterministic algorithm obtains significantly higher CRs under the same conditions because it ignores the cost of the randomness caused by the REPG and load. Therefore, the time-series simulation based on RO can provide more accurate learning samples for RBFNN training.

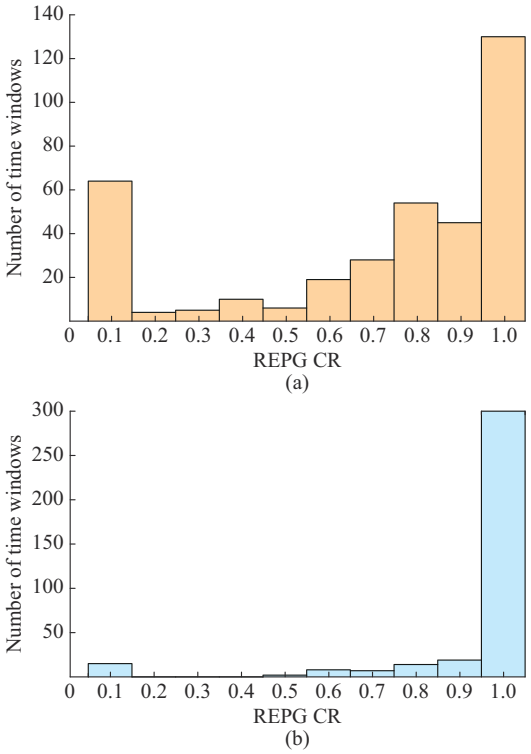

Fig. 8. Histograms of CRs in various time windows. (a) RO. (b) Deterministic algorithm.

The simulation period is adjustable. Thus, by adjusting the duration and number of time windows, the REPG absorption results of this the modified IEEE 14-bus system for different periods can be obtained.

B. Application of AFSA-RBFNN

We achieve different results of REPG absorption with various parameters through time-series simulation based on RO, which provides training and test samples for the RBFNN. The value ranges of the parameters are shown in Table I, where the value of PVDL is the ratio of PL to valley load, while the values of MICG and RRCG indicate the corresponding ratios of CCG.

TABLE I
VALUE RANGES OF PARAMETERS

Parameter	Value range
PEL	±4%-±10%
PL	210-300 MW
PVDL	1.1-1.4
AFL	0-40 MW
TLC	65-85 MW
REC	70-110 MW
PERE	±4%-±10%
CCG	220-300 MW
MICG	0.1-0.5
RRCG	0.2-0.6

Within the value ranges of parameters, 900 different data sets are randomly selected as the input of the time-series simulation based on RO, which takes approximately 48 hours to complete. Figure 9 presents the negative correlation between the REPG CR and constraint violation rate (CVR), which is defined as the ratio of time windows during which the constraints cannot be satisfied to the total number of time windows.

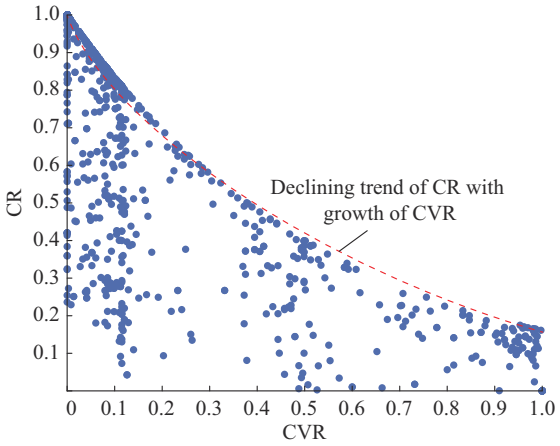

Fig. 9. Negative correlation between REPG CR and CVR.

Seventy percentage of the results from the time-series simulation are randomly selected as the training set, while the remaining 30% are used as the test set. The AFSA is adopted to train the RBFNN, while another NN with a tansig activation function is trained by the error back propagation NN (BPNN) as a control. The parameters of the AFSA are set as follows: the number of artificial fishes is 30, the maximum number of attempts is 10, the vision is 2, the step size is 0.5, and the crowding factor is 0.618. We present the structures of the RBFNN trained by the AFSA and BPNN in Fig. SA4 of Supplementary Material. All the NNs are implemented based on MATLAB.

The performance of different algorithms on the training set is shown in Table II. The training time of the RBFNN

based on the iterative method is the shortest, but this NN has the most significant mean square error (MSE), which can be significantly reduced based on the AFSA through a longer training time. The MSE of BPNN in the training set is also acceptable, and it has half the training time of the AFSA-RBFNN.

TABLE II
PERFORMANCE OF DIFFERENT ALGORITHMS ON TRAINING SET

Algorithm	MSE	Training time (s)
BPNN	0.0030	4.070
RBFNN	0.0150	0.741
AFSA-RBFNN	0.0013	11.797

The comparison of performance on test set between AFSA-RBFNN and BPNN is illustrated in Fig. 10. The RBFNN performs significantly better on the test set than the BPNN. The MSE of AFSA-RBFNN is 0.0027 and 0.0026 when predicting CR and CVR, respectively.

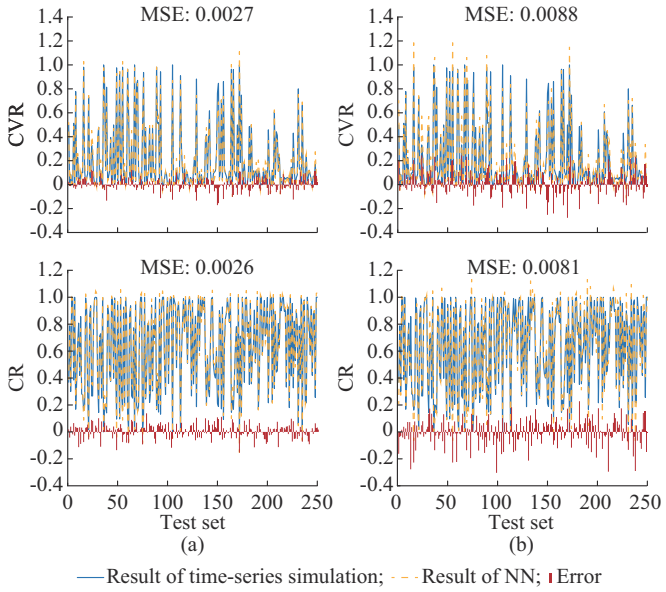

Fig. 10. Comparison of performance on test set between AFSA-RBFNN and BPNN. (a) AFSA-RBFNN. (b) BPNN.

To further demonstrate the advantages of AFSA-RBFNN in the application scenarios of this paper, we gradually increase the number of neurons in the hidden layer of BPNN from 10 to 60. Figure 11 shows MSE of BPNN on the training and test sets. As the number of neurons increases, BPNN performs better and obtains lower MSE on the training set. However, on the test set, the performance of BPNN has not surpassed AFSA-RBFNN. On the contrary, when the number of neurons exceeds 40, MSE tends to increase because of overfitting.

C. Global Sensitivity Analysis

Generate 100000 sets of parameters within the ranges in Table I, then input them to the trained RBFNN, and we can obtain the absorption results. On this basis, the influence of each parameter on absorption is analyzed by employing Sobol' method.

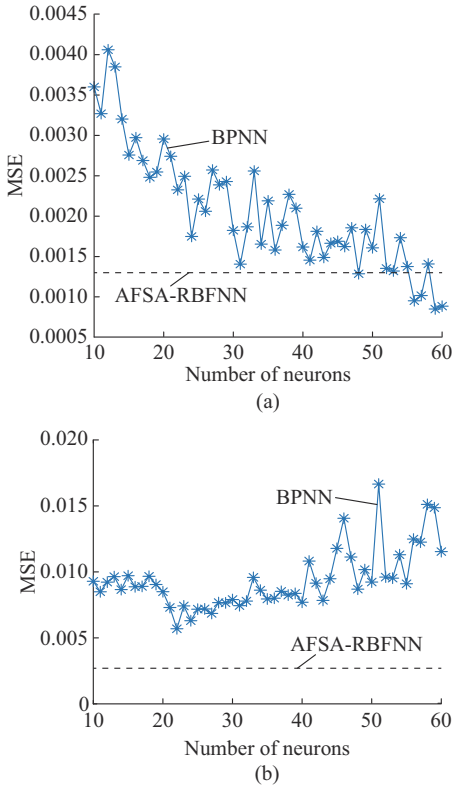

Fig. 11. MSE of BPNN on training and test sets. (a) Training set. (b) Test set.

Figure 12(a) and (b) presents the results of global sensitivity analysis of CVR and CR to different parameters, respectively. The parameters with large total sensitivity coefficients can influence the absorption results more significantly, so they should be adjusted first if there is an unexpected curtailment of the REPG.

According to Fig. 12, the peak regulation capacity of conventional generations (MICG and RRCG), whose total sensitivity coefficients are significantly higher than others, has the most critical impact on REPG absorption. Therefore, expanding the adjustment ranges of the maximum/minimum output of conventional units can create more space for the REPG absorption when ensuring the balance of the power system. In addition, flexible load also has a significant promotion effect on absorption results. Besides, we cannot ignore the limitation of the TLC.

D. Discussion

1) The time-series simulation based on RO obtains a lower CR than deterministic optimization due to the strict restriction of uncertainty. The results of the stochastic optimization are supposed to be bounded between them. Rather than the scheduling plan, this paper estimates the REPG and analyzes the key factors affecting absorption. Therefore, the time-series simulation based on RO, which can account for various parameters, is suitable for this application scenario and can provide high-quality learning samples for RBFNN training.

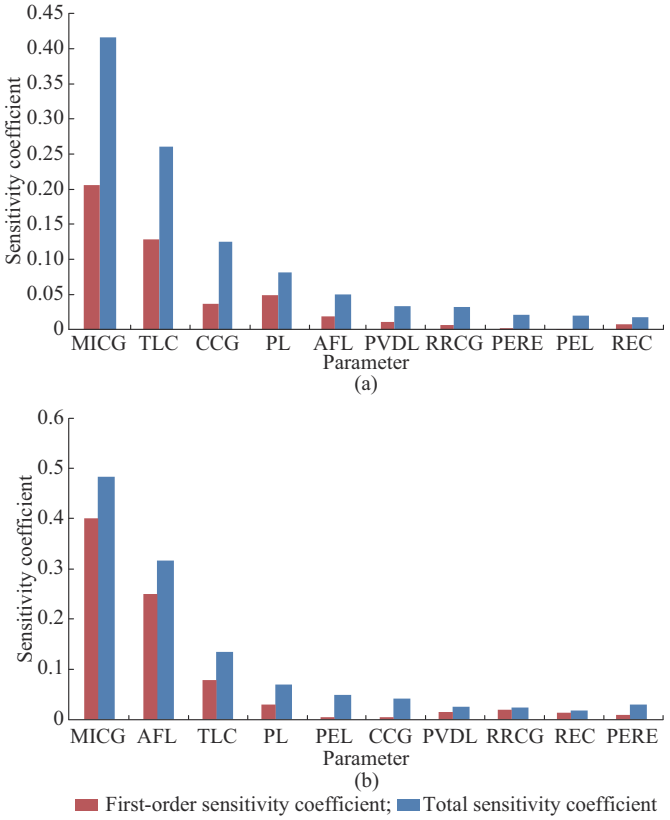

Fig. 12. Results of global sensitivity analysis of CVR and CR to different parameters. (a) CVR. (b) CR.

2) BPNN and AFSA-RBFNN have their advantages in the training set. However, the performance of the AFSA-RBFNN is significantly better on the test set, which proves its strong generalization ability. This ability comes from the characteristics of RBFNN and the underlying mathematical relationship between input parameters and absorption results. It is difficult for the NN to obtain the absorption results entirely consistent with the time-series simulation. In contrast, it enables the operators to quickly perceive the REPG absorption situation in real time since the calculation time of the trained RBFNN is less than 1 ms. On the test set, the Pearson correlation coefficients between the results of RBFNN and the time-series simulation are close to 1 (0.9882 and 0.9839), i.e., they have incredibly high consistency.

3) We find that the first-order sensitivity coefficients of most parameters are much smaller than the total sensitivity coefficients, especially parameters such as PERE, REL, and CCG. It illustrates that although the independent influence of these parameters is small, they can also change the absorption results by coupling with other parameters. The discovery of this hidden relationship is also the significance of the global sensitivity analysis.

VI. Conclusion

This paper proposes an architecture combining the AFSA-RBFNN and the time-series simulation based on RO for online SA and sensitivity analysis of the REPG absorption. First, RO is adopted to consider the influence of the uncertainties of REPG and grid load. The calculation results are more suitable for analyzing the absorption expectation. Then, we introduce the RBFNN trained by AFSA to effectively fit the input-output relationship of the time-series simulation based on RO, making it possible to conduct the online SA of the REPG absorption with different parameters within the specified power grid and period.

The global sensitivity analysis based on Sobol' method shows that the peak regulation capacity of conventional generations, TLC, and flexible load significantly impacts the absorption results.

The trained RBFNN and sensitivity analysis results apply to the given power grid and period. However, this analysis procedure described in this paper is universal, i.e., online applications in different times and spaces using NNs can be supported by their corresponding offline time-series simulations.

References

[1] Y. Wolde-Rufael and E. M. Weldemeskel, "Environmental policy stringency, renewable energy consumption and CO_2 emissions: panel cointegration analysis for BRIICTS countries," *International Journal of Green Energy*, vol. 17, no. 10, pp. 568-582, Aug. 2020.

[2] S. Ma, L. Lu, H. Zhang *et al*., "Multi-regions bundled planning of wind farm, thermal, energy storage with renewable energy consumption," in *Proceedings of 2021 3rd Asia Energy and Electrical Engineering Symposium (AEEES)*, Chengdu, China, Mar. 2021, pp. 1130-1135.

[3] J. Zhu, Y. Yuan, and W. Wang, "Multi-stage active management of renewable-rich power distribution network to promote the renewable energy consumption and mitigate the system uncertainty," *International Journal of Electrical Power & Energy Systems*, vol. 111, no. 1, pp. 436-446, Oct. 2019.

[4] R. Palma-Behnke, F. Valencia, J. Vega-Herrera *et al*., "Synthetic time series generation model for analysis of power system operation and expansion with high renewable energy penetration," *Journal of Modern Power Systems and Clean Energy*, vol. 9, no. 4, pp. 849-858, Jul. 2021.

[5] A. Q. Al-Shetwi, M. A. Hannan, K. P. Jern *et al*., "Grid-connected renewable energy sources: review of the recent integration requirements and control methods," *Journal of Cleaner Production*, vol. 253, p. 119831, Apr. 2020.

[6] Y. Yasuda, L. Bird, E. M. Carlini *et al.*, "C-E (curtailment-energy share) map: an objective and quantitative measure to evaluate wind and solar curtailment," *Renewable and Sustainable Energy Reviews*, vol. 160, p. 112212, Feb. 2022.

[7] F. Liu, X. Zhang, N. Li *et al.*, "Research on optimal matching scheme of renewable energy based on renewable energy consumption ability," in *Proceedings of IEEE Conference on Energy Internet and Energy System Integration (EI2)*, Beijing, China, Oct. 2018, pp. 1-6.

[8] A. Yazdaninejadi, A. Hamidi, S. Golshannavaz *et al*., "Impact of inverter-based DERs integration on protection, control, operation, and planning of electrical distribution grids," *The Electricity Journal*, vol. 32, vol. 6, pp. 43-56, Jul. 2019.

[9] W. Xuan, H. Li, Z. Liu *et al.*, "Urban renewable energy consumption capacity quantitative and improving approach," in *Proceedings of IEEE Student Conference on Electrical Machines and Systems (SCEMS)*, Jinan, China, Dec. 2020, pp. 853-857.

[10] Q. Xu, C. Kang, N. Zhang *et al*., "A probabilistic method for determining grid-accommodable wind power capacity based on multi-scenario system operation simulation," *IEEE Transactions on Smart Grid*, vol. 7, no. 1, pp. 400-409, Jan. 2016.

[11] H. Zhou, H. Wu, C. Ye *et al*., "Integration capability evaluation of wind and photovoltaic generation in power systems based on temporal and spatial correlations," *Energies*, vol. 12, no. 1, pp. 1-12, Jan. 2019.

[12] W. Zhang, H. Qiu, and S. Sheng, "Comprehensive assessment method of new energy consumption considering steady and dynamic active power equilibrium constraints," in *Proceedings of International Conference on Automation, Mechanical and Electrical Engineering (AMEE)*, Shanghai, China, Jul. 2018, pp. 474-482.

[13] Z. Zhang, W. Wang, G. Zhang *et al*., "Assessment method of accommodation capacity of renewable energy based on non-time-series model," *Automation of Electric Power Systems*, vol. 43, no. 20, pp. 24-32, Dec. 2019.
[14] M. Fan, V. Vittal, G. T. Heydt *et al*., "Probabilistic power flow studies for transmission systems with photovoltaic generation using cumulants," *IEEE Transactions on Power Systems*, vol. 27, no. 4, pp. 2251-2261, Nov. 2012.
[15] M. Aienab, A. Hajebrahimic, and M. Fotuhi-Firuzabad, "A comprehensive review on uncertainty modeling techniques in power system studies," *Renewable and Sustainable Energy Reviews*, vol. 57, no. 1, pp. 1077-1089, May 2016.
[16] C. Liu, J. Qu, and W. Shi, "Evaluating method of ability of accommodating renewable energy based on probabilistic production simulation," *Chinese Journal of Electrical Engineering*, vol. 40, no. 10, pp. 3134-3144, Mar. 2020.
[17] L. Ye, C. Zhang, H. Xue *et al.*, "Study of assessment on capability of wind power accommodation in regional power grids," *Renewable Energy*, vol. 133, no. 1, pp. 647-662, Apr. 2019.
[18] E. Nycander, L. Södera, J. Olauson *et al*., "Curtailment analysis for the Nordic power system considering transmission capacity, inertia limits and generation flexibility," *Renewable Energy*, vol. 152, no. 1, pp. 942-960, Jun. 2020.
[19] C. Sun, Z. Bie, and Z. Zhang, "A new framework for the wind power curtailment and absorption evaluating," *International Transactions on Electrical Energy Systems*, vol. 26, no. 10, pp. 2134-2147, Oct. 2016.
[20] H. Li, N. Zhang, C. Kang *et al.*, "Analytics of contribution degree for renewable energy accommodation factors," *Proceedings of the CSEE*, vol. 39, no. 4, pp. 1009-1017, Feb. 2019.
[21] X. Li, Y. Wang, Y. Huang *et al.*, "Research on the quantitative evaluation method of wind power and photovoltaic power curtailment in real-time market transactions," in *Proceedings of International Conference on Power System Technology (POWERCON)*, Guangzhou, China, Nov. 2018, pp. 1564-1572.
[22] J. Zhu, K. Shi, Q. Li *et al.*, "Time series production simulation and renewable energy accommodation capacity evaluation considering transmission network power flow constraints," *Power System Technology*, vol. 46, no. 5, pp. 1947-1955, May 2022.
[23] M. Panteli and D. S. Kirschen, "Situation awareness in power systems: theory, challenges and applications," *Electric Power Systems Research*, vol. 122, no. 1, pp. 140-151, May 2015.
[24] S. Nitish, H. Geoffrey, K. Alex *et al.*, "Dropout: a simple way to prevent neural networks from overfitting," *Journal of Machine Learning Research*, vol. 15, no. 1, pp. 1929-1958, Jun. 2014.
[25] D. Efimov and H. Sulieman, "Sobol sensitivity: a strategy for feature selection," in *Proceedings of International Conference on Mathematics and Statistics (ICMS)*, Sharjah, United Arab Emirates, Apr. 2015, pp. 57-75.
[26] C. Zhao, J. Wang, J. P. Watson *et al.*, "Multi-stage robust unit commitment considering wind and demand response uncertainties," *IEEE Transactions on Power Systems*, vol. 28, no. 3, pp. 2708-2717, Aug. 2013.
[27] Z. Zhang, Z. Chen, Q. Zhao *et al*., "Multi-level cooperative scheduling based on robust optimization considering flexibilities and uncertainties of ADN and MG," *Energies*, vol. 14, no. 21, pp. 7376-7398, Nov. 2021.
[28] H. Zhou, Y. Zhou, J. Hu *et al*., "LSTM-based energy management for electric vehicle charging in commercial-building prosumers," *Journal of Modern Power Systems and Clean Energy*, vol. 9, no. 5, pp. 1205-1216, Sept. 2021.
[29] M. Mohammed and G. V. M. Istemihan, "Post-fault prediction of transient instabilities using stacked sparse autoencoder," *Electric Power Systems Research*, vol. 164, no. 1, pp. 243-252, Nov. 2018.
[30] F. Fernandez-Navarro, C. Hervas-Martinez, P. A. Gutierrez *et al.*, "Generalised Gaussian radial basis function neural networks," *Soft Computing*, vol. 17, no. 3, pp. 519-533, Mar. 2013.
[31] T. Xie, H. Yu, and B. Wilamowski, "Comparison between traditional neural networks and radial basis function networks," in *Proceedings of IEEE International Symposium on Industrial Electronics (ISIE)*, Gdansk, Poland, Jun. 2011, pp. 1194-1199.
[32] R. Kumar, S. Srivastava, and J. R. P. Gupta. "Time series prediction using focused time lagged radial basis function network," in *Proceedings of International Conference on Information Technology (InCITe)*, Noida, India, Oct. 2016, pp. 121-124.
[33] D. Yu and D. Yu, "Neural network control of multivariable processes with a fast optimisation algorithm," *Neural Computing & Applications*, vol. 12, no. 1, pp. 3-4, Dec. 2003.
[34] Z. Zhang, "Pattern classification based on radial basis function neural network," in *Proceedings of International Conference on Smart Grid and Electrical Automation (ICSGEA)*, Zhangjiajie, China, Jun. 2020, pp. 213-216.
[35] W. Shen, X. Guo, C. Wu *et al.*, "Forecasting stock indices using radial basis function neural networks optimized by artificial fish swarm algorithm," *Knowledge-based Systems*, vol. 24, no. 3, pp. 378-385, Apr. 2011.
[36] Z. Huang and Y. Chen, "Log-linear model-based behavior selection method for artificial fish swarm algorithm," *Computational Intelligence and Neuroscience*, vol. 2015, no. 10, pp. 1-10, Jan. 2015.
[37] J. Nossent, P. Elsen, and W. Bauwens, "Sobol' sensitivity analysis of a complex environmental model," *Environmental Modelling & Software*, vol. 26, no. 12, pp. 1515-1525, Dec. 2011.
[38] X. Xu, Z. Yan, M. Shahidehpour *et al.*, "Power system voltage stability evaluation considering renewable energy with correlated variabilities," *IEEE Transactions on Power Systems*, vol. 33, no. 3, pp. 3236-3245, May 2018.
[39] K. N. Hasan and R. Preece, "Influence of stochastic dependence on small-disturbance stability and ranking uncertainties," *IEEE Transactions on Power Systems*, vol. 33, no. 3, pp. 3227-3235, May 2018.
[40] G. Mavromatidis, K. Orehounig, and J. Carmeliet, "Uncertainty and global sensitivity analysis for the optimal design of distributed energy systems," *Applied Energy*, vol. 214, no. 1, pp. 219-238, Mar. 2018.

Ziqi Zhang received the B.Sc. degree from the College of Electrical Engineering, Wuhan University, Wuhan, China, in 2016, and the M.Sc. degree from the School of Electrical Engineering, Southeast University, Nanjing, China, in 2019, where he is currently pursuing the Ph.D. degree in electrical engineering in Southeast University. His research interests include the integration of flexible load and renewable energy into modern power systems and application of artificial intelligence to engineering.

Zhong Chen received the M.Sc. and Ph.D. degrees from the School of Electrical Engineering, Southeast University, Nanjing, China, in 2002 and 2006, respectively. He is currently a Full Professor with Southeast University, and was a Senior Visiting Scholar at the University of Bath, Bath, UK, and Queen's University Belfast, Belfast, UK, from 2006 to 2007. He now serves as the Vice-chairman of the IEEE PES Power Grid Stability Control Technology Subcommittee. His research interests include electric vehicles, renewable energy, and integrated power system operation and control.

Qi Zhao received the B.Sc. degree in electrical power system and automation from Nanjing Institute of Technology, Nanjing, China, in 2013. Currently, he serves as an Engineer at the Suzhou Power Supply Branch of the State Grid Jiangsu Electric Power Company, Suzhou, China. His research interest includes situation awareness of urban power grid.

Yi Wang received the B.Sc. and M.Sc. degrees from Hohai University, Nanjing, China, in 2002 and 2009, respectively. He is a Senior Engineer at NARI Group Corporation Ltd. (State Grid Electric Power Research Institute Ltd.), Nanjing, China. His research interests include power system regulation and optimization.

Jiang Tian received the B.Sc. degree in electrical engineering from Shanghai Jiao Tong University, Shanghai, China, in 2004, and the M.Sc. degree from Suzhou University, Suzhou, China, in 2011. He is a Senior Engineer at the Suzhou Power Supply Branch of State Grid Jiangsu Electric Power Co., Ltd., Suzhou, China. His research interests include operation and sensitivity analysis of urban power grid.